A numerical study of nonlinear Schrödinger equation solutions for microwave solitons in magnetic thin films

Ming Chen, Jon M. Nash, and Carl E. Patton
Department of Physics, Colorado State University, Fort Collins, Colorado 80523

(Received 27 April 1992; accepted for publication 4 January 1993)

Dipole-exchange spin wave pulses in magnetic thin films have been numerically modeled with the nonlinear Schrödinger equation. Small input pulse amplitudes yield propagating wave packets which exhibit a linear response. As the amplitude of the input pulse is increased, the propagating spin-wave pulse exhibits soliton and then multisoliton structures. In the soliton regime, three principal characteristics are observed. First, in the zero damping limit, the soliton propagates without changing its shape. Second, the soliton exhibits an inherent velocity in addition to its linear group velocity. Third, the soliton exhibits a damping rate that is approximately twice that in the linear regime.

I. INTRODUCTION

The nonlinear Schrödinger (NLS) equation has been used to describe a variety of nonlinear phenomena in plasma and optical physics.[1–4] Nonlinear dipole-exchange spin wave wave packets in single crystal yttrium iron garnet (YIG) magnetic thin films are also observed to have envelope soliton characteristics which can be modeled by the nonlinear Schrödinger equation.[5–7] Because magnetic thin films have unique characteristics it is necessary to study the numerical solutions of the nonlinear Schrödinger equation in this context. A detailed study of selected numerical solutions for parameters, which match typical thin film experiments, has been made in order to better understand soliton theory and to better model microwave magnetic soliton profiles. These solutions were obtained using a forward time centered space implicit scheme.[8,9] It is shown that the shape and structure of the wave packet depend strongly on the amplitude of the input pulse. Results are also given which have not been previously demonstrated for magnetic media. In the soliton regime the wave packet propagates with an increased velocity and an increased damping rate. In the zero damping limit, the soliton propagates without changing shape. The formation of solitons is empirically observed to occur only when the dispersion and the nonlinear terms in the NLS equation are of opposite sign, as predicted from soliton theory.[10,11]

II. NONLINEAR SCHRÖDINGER EQUATION

Consider a general wave packet like microwave magnetization response $m(x,t)\exp[i(kx-\omega t)]$, where ω and k are the frequency and wave number for a chosen thin film dipole-exchange spin-wave mode and $m(x,t)$ is the microwave magnetization amplitude response. The nonlinear response is given by solutions to the so-called nonlinear Schrödinger equation,[5]

$$i\left(\frac{\partial U}{\partial t}+\omega_k'\frac{\partial U}{\partial x}+\eta U\right)+\frac{1}{2}\omega_k''\frac{\partial^2 U}{\partial x^2}-N|U|^2U=0. \quad (1)$$

In the above $U=U(x,t)$ is the normalized response defined by $U=m(x,t)/(\sqrt{2}M_s)$, where M_s is the saturation magnetization of the material. The coefficients ω_k' and ω_k'' are the first and second order partial derivatives of the nominal spin-wave frequency ω with respect to the wave number k, respectively, for the chosen (ω,k) mode. The parameter ω_k' is the group velocity for the linear wave packets. The parameter ω_k'' relates to the dispersion of the medium. The parameter η is the spin wave relaxation rate which characterizes losses in the material. The parameter N is the derivative of the spin wave frequency with respect to $|U|^2$, $\partial\omega/\partial|U|^2$, and is the coefficient of the nonlinear term in Eq. (1). When the amplitude U is small, this term can be neglected.

The physical content of Eq. (1) can be better understood if the essential terms are written in standard Schrödinger equation format,

$$-i\frac{\partial U}{\partial t}=\frac{1}{2}\omega_k''\frac{\partial^2 U}{\partial x^2}-N|U|^2U. \quad (2)$$

The term on the left is a total energy term. The first term on the right is a kinetic energy-like term. The second term on the right hand side is a potential energy-like term which depends on the function U. It is this U dependence which makes the equation nonlinear. The remaining ω_k' and η terms in Eq. (1) serve to introduce spatial propagation and damping.

One may solve Eq. (1) in several ways. First, in the limit of zero damping, one can use one of the several analytic solutions. When the parameter N is greater than zero and the parameter ω_k' is less than zero, an exact single-soliton solution to Eq. (1) is given by[10]

$$U_a(x,t)=\beta\sqrt{2/N}\ \mathrm{sech}\ (f)e^{i\theta}, \quad (3)$$

where the f and θ functions are defined by

$$f=\beta\sqrt{2/|\omega_k''|}\,(x-x_0-\omega_k't)+2\beta\xi t, \quad (4)$$

and

$$\theta=\xi\sqrt{2/|\omega_k''|}\,(x-\omega_k't)+(\xi^2-\beta^2)t+\varphi_0. \quad (5)$$

Recall that the $\exp[i(kx-\omega t)]$ spin wave carrier response has already been factored out of the solution. The $\mathrm{sech}(f)$ term describes the wave packet envelope function for the soliton. The $\exp(i\theta)$ term represents a space and time de-

 0021-8979/93/083906-04$06.00

pendent phase. The β parameter controls the amplitude and width of the envelope function. The ξ parameter controls the soliton envelope velocity v_e.

$$v_e=\omega_k'-2\xi\sqrt{|\omega_k''|/2}. \tag{6}$$

For the case of nonzero damping, exact solutions to Eq. (1) are not available. An approximate single-soliton solution to Eq. (1) under the condition of weak damping can be obtained using perturbation methods[12,13] and is given by

$$\tilde{U}_a(x,t)=\beta e^{-2\eta t}\sqrt{2/N}\,\mathrm{sech}(\,fe^{-2\eta t})e^{i\tilde{\theta}}, \tag{7}$$

with

$$\tilde{\theta}=\xi\sqrt{2/|\omega_k''|}\,(x-\omega_k't)+\xi^2t-\beta^2(1/4\eta)(1-e^{-4\eta t})+\varphi_0. \tag{8}$$

It is clear from Eq. (7) that the soliton envelope decays exponentially at a rate which is twice the linear relaxation rate η. From the f factor in Eq. (7), it is also clear that the envelope velocity v_e is not affected by the damping.

One may also proceed to solve Eq. (1) by numerical techniques. In doing so, one has many possible choices of initial conditions and boundary conditions. Two have been selected for the present purposes. The first such set of initial conditions and boundary conditions is based on the simple analytic solution presented above

$$U(x,0)=U_a(x,0), \tag{9a}$$

$$U(\pm L,t)=0. \tag{9b}$$

The starting pulse is positioned at $x_0=0$. These conditions, along with reasonable values of ξ and β, were used to generate propagating pulses for comparison with the analytic solution described above, and to study the effects of damping on soliton profiles.

The second such set of initial and boundary conditions is based on the more typical initial conditions in real magnetic thin film soliton experiments. Here, one simply uses a square pulse applied at $x_0=0$

$$U(0,t)=\begin{cases}U_0, & 0<t\leqslant\tau;\\ 0, & \text{elsewhere},\end{cases} \tag{10a}$$

$$U(L,t)=0, \tag{10b}$$

$$U(x,0)=0, \quad 0\leqslant x\leqslant L. \tag{10c}$$

Here, U_0 is the amplitude of the starting pulse and τ is the pulse width. In both scenarios, we limit our examination to x values which satisfy $x\ll L$ in the numerical procedure.

III. NUMERICAL RESULTS

Soliton envelope profiles based on the sech-shaped pulse initial conditions and boundary conditions in Eq. (9) are shown in Fig. 1. The NLS equation parameters were set as follows: $\omega_k'=0$, $\omega_k''=-2.0\ \mathrm{cm}^2/\mu\mathrm{s}$, $N=2\ \mu\mathrm{s}^{-1}$. The initial sech(f) parameters were: $\beta=2\ \mu\mathrm{s}^{-1/2}$, $x_0=0$, $\xi=-2\ \mu\mathrm{s}^{-1/2}$, and $\varphi_0=0$. These parameter values were chosen for numerical convenience. They also correspond to reasonable values for thin film soliton experiments.

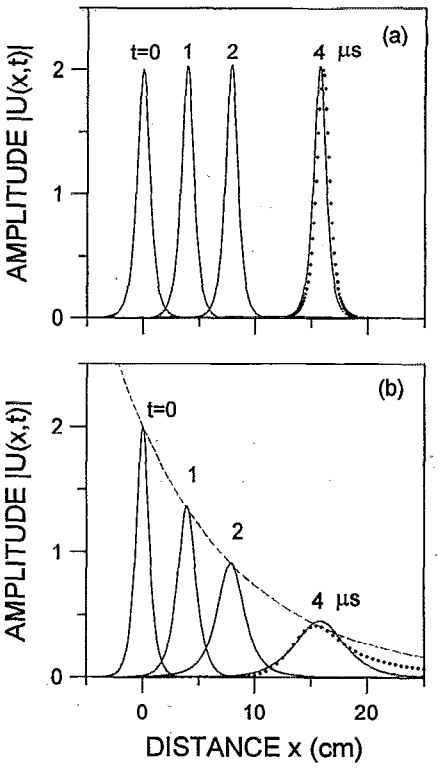

FIG. 1. Numerical results for a propagating sech-type soliton pulse with (a) zero damping and (b) nonzero damping with $\eta=0.2\ \mu\mathrm{s}^{-1}$. The dotted profiles are plots of the analytic solutions at $t=4\ \mu$s. The dashed curve in (b) shows exponential decay according to $\exp[-2\eta t]$.

The solid line pulses in Fig. 1(a) show numerical soliton solutions for $t=1$, 2, and 4 μs, based on starting conditions given by Eq. (9) at $t=0$ and the parameters given above. The damping parameter η is set to zero. The numerical results show a single sech-like envelope which propagates at a velocity $v_e=4$ cm/μs and without attenuation or change in shape. The observed velocity matches the analytic result in Eq. (6). It is to be emphasized that these solutions are for a linear spin wave group velocity $\omega_k'=0$. Even in this $\omega_k'=0$ limit the nonlinear pulses have a well defined nonzero velocity. The pulse indicated by the dotted curve in Fig. 1(a) shows the analytic result for $t=4$ μs. The numerical result at $t=4$ μs is in reasonable agreement with the analytic curve. We see, therefore, that (a) the present numerical procedure yields NLS equation soliton solutions which agree with analytic solutions and (b) solitons propagate without change of shape at a well defined velocity even in the $\omega_k'=0$ limit.

Figure 1(b) shows the additional effect of damping. The four profiles shown as solid curves in Fig. 1(b) were obtained as for Fig. 1(a), except that the relaxation rate η was increased to $\eta=0.2\ \mu\mathrm{s}^{-1}$, which corresponds to a ferromagnetic resonance linewidth of 0.023 Oe. These values were chosen to illustrate the effect of soliton decay on a reasonable scale. Actual linewidths and η values for YIG are an order of magnitude larger. The inclusion of damping causes the pulse amplitude to decrease with propagation distance and pulse broadening. The decay length of about

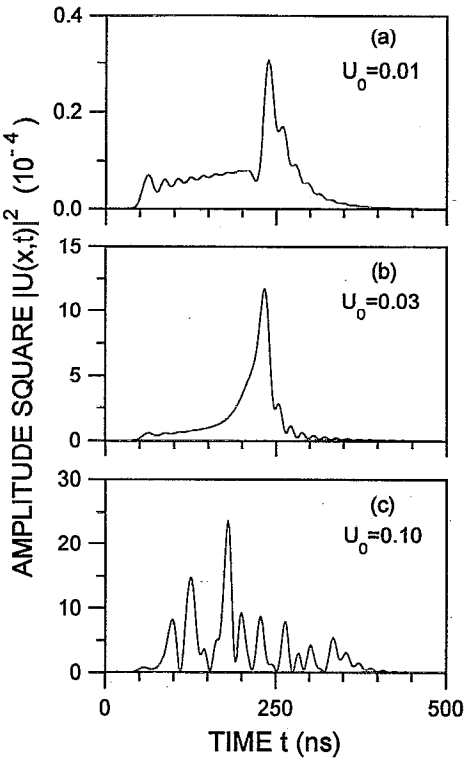

FIG. 2. Numerical results for propagating spin wave profiles generated in a YIG thin film at $x=0.4$ cm with a square 180 ns input pulse at $x=0$.

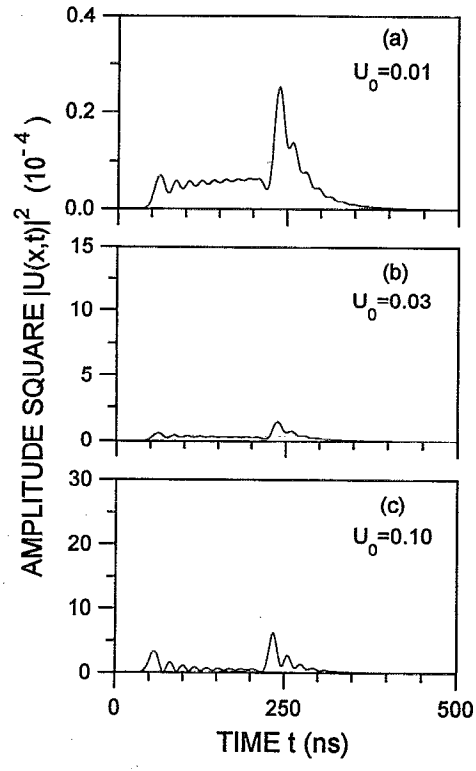

FIG. 3. Numerical results for propagating spin wave profiles generated in a YIG thin film at $x=0.4$ cm with a square 180 ns input pulse at $x=0$ and $\omega_k''=0.3$ cm$^2/\mu$s.

10 cm evident from Fig. 1(b) corresponds to a decay time of 2.5 μs, based on the envelope velocity $v_e=4$ cm/μs. This corresponds to a decay rate of 0.4 μs^{-1}, which is twice the relaxation rate η. The dashed curve in Fig. 1(b) shows exponential decay according to $\exp[-2\eta t]$. For comparison, the approximate solution given by Eq. (7) for $t=4$ μs is shown in Fig. 1(b) by the dotted curve. The differences between the solid line numerical solution and the dotted curve approximate solution are clearly evident. We see that while damped solitons do not really propagate without change of shape, they do evidence a decay rate which is approximately double the intrinsic relaxation rate in the linear regime.

Soliton envelope profiles based on the square pulse initial conditions and boundary conditions in Eq. (10) are shown in Fig. 2. The NLS equation parameters were set to: $\omega_k'=1.8$ cm/μs, $\eta=6.0$ μs^{-1}, $\omega_k''=-0.3$ cm$^2/\mu$s, and $N=3.0\times10^4$ μs^{-1}. This particular choice of NLS equation parameters corresponds to a perpendicularly magnetized 5.8 μm YIG film with pinned surface spins and a specific dipole-exchange spin wave at $\omega=4.437$ GHz and $k=2.3\times10^2$ cm^{-1}. These are the same operating conditions used in the thin film soliton experiments of Kalinikos *et al.*[6]

The results given in Fig. 2 are for $x=0.4$ cm with the square input pulse applied at $x=0$ as in Eq. (10). Profiles were calculated for a normalized input pulse of amplitude U_0 increasing from 0 to 0.10 with a fixed pulse duration of 180 ns. The results show the transition of the excited spin waves from the linear to nonlinear regime, and from a single soliton pulse to a multiple soliton structure. Figure 2(a) shows the linear response obtained at $U_0=0.01$. One finds the same response, albeit at reduced amplitude, for $U_0\leqslant0.01$. The onset of nonlinear behavior in the spin wave response is demonstrated in Fig. 2(b). The input pulse at $U_0=0.03$ yields a propagating pulse which differs markedly from the linear response in Fig. 2(a). The peak of the spin wave pulse narrows and the shape changes to a single soliton type profile. Figure 2(c) shows the effect of an even larger input pulse, $U_0=0.10$. The profile now shows a multiple soliton type structure. We see that (a) the excited spin wave pulse exhibits a response similar to that expected in the linear regime when the initial pulse amplitude is small, (b) when the input pulse amplitude is increased the excited pulse narrows and sharpens into a single soliton type profile, and (c) at larger input pulse amplitudes the excited pulse widens and separates into several distinct soliton shaped peaks.

Figure 3 shows the results of solving Eq. (1) with the conditions and parameter values given above but with the ω_k'' parameter changed from -0.3 to $+0.3$ cm$^2/\mu$s. The effect of this change is to move from the soliton supporting side of the spin-wave dipole-exchange dispersion gap to the other side of the gap for which solitons are not supported. The three profiles in Fig. 3 were calculated for the same spatial positions and input pulse amplitudes as in Fig. 2 and plotted with the same scales used for the three profiles in Fig. 2, respectively.

A comparison of the profiles in Fig. 3 with their counterparts in Fig. 2 reveals several interesting results. First, the response to the input pulse at higher U_0 levels has been significantly reduced by the change in sign of the ω_k'' term. Second, the profiles in Fig. 3 all have a shape which is similar to the shape of the linear response shown in Fig. 2(a). Third, none of the profiles in Fig. 3 exhibit the strong nonlinear response or the multiple peak structure seen in Fig. 2. In fact, all the profiles in Fig. 3 represent responses that are essentially linear to the input amplitude. We see therefore, that when the dispersion coefficient is positive no solitons are formed, regardless of the input pulse amplitude. This is in agreement of the criterion obtained by Zakharov and Shabat[10,11] for NLS equation solitons.

IV. CONCLUSION

The nonlinear Schrödinger equation has been used to numerically model the spatial propagation of microwave envelope solitons in magnetic thin films. By applying the model to a known analytic soliton solution of the NLS equation, three soliton characteristics were observed. First, for zero damping the shape of the soliton is seen to remain constant in time. Second, the soliton is observed to propagate with an intrinsic velocity that is predicted by theory. Third, when the damping is nonzero, the soliton is damped at a rate which is approximately twice that expected for a linear spin wave pulse. More complicated soliton solutions were obtained by using time dependent boundary conditions which mimic conditions in microwave pulse experiments. The results from their calculations show that soliton formation is dependent on the initial pulse amplitude and the sign of the dispersion. As the input power level is increased the shape of the spin wave pulse changes from a linear to a soliton shape, and finally to a multisoliton type shape. These results agree qualitatively with those obtained experimentally.

ACKNOWLEDGMENTS

The authors would like to thank Dr. M. J. Ablowitz for helpful discussions. This work was supported in part by the National Science Foundation grant No. DMR-8921761 and by the U.S. Army Research Office grant No. DAAL03-91-G-0327.

[1] A. Hasegawa, *Plasma Instabilities and Nonlinear Effects* (Springer, New York, 1975), p. 194.
[2] F. F. Chen, *Introduction to Plasma Physics and Controlled Fusion*, 2nd ed. (Plenum, New York, 1984), Vol. 1, p. 336.
[3] M. J. Ablowitz and H. Segur, *Solitons and the Inverse Scattering Transformation* (SIAM, Philadelphia, 1981), p. 312.
[4] A. Hasegawa, *Optical Solitons in Fibers*, 2nd ed. (Springer, Berlin, 1990).
[5] A.K. Zvezdin and A. F. Popkov, Zh. Eksp. Teor. Fiz. **84**, 606 (1983) [Sov. Phys. JETP **57**, 350 (1983)].
[6] B. A. Kalinikos, N. G. Kovshikov, and A. N. Slavin, J. Appl. Phys. **67**, 5633 (1990).
[7] A. N. Slavin and G.M. Dudko, J. Magn. Magn. Mater. **86**, 115 (1990).
[8] M. Delfour, M. Fortin, and G. Payre, J. Comput. Phys. **44**, 277 (1981).
[9] T. R. Taha and M. J. Ablowitz, J. Comput. Phys. **55**, 203 (1984).
[10] V. E. Zakharov and A. B. Shabat, Zh. Eksp. Teor. Fiz. **61**, 118 (1971) [Sov. Phys. JETP **34**, 62 (1972)].
[11] V. E. Zakharov and A. B. Shabat, Zh. Eksp. Teor. Fiz. **64**, 1627 (1973) [Sov. Phys. JETP **37**, 823 (1973)].
[12] Y. Kodama and M. J. Ablowitz, Stud. Appl. Math. **64**, 225 (1981).
[13] G. L. Lamb, *Elements of Soliton Theory* (Wiley, New York, 1980), p. 275.